

Document downloaded from:

<http://hdl.handle.net/10251/75091>

This paper must be cited as:

Ortega-Toro, R.; Morey, I.; Talens Oliag, P.; Chiralt A. (2015). Active bilayer films of thermoplastic starch and polycaprolactone obtained by compression molding. *Carbohydrate Polymers*. 127:282-290. doi:10.1016/j.carbpol.2015.03.080.



The final publication is available at

<http://dx.doi.org/10.1016/j.carbpol.2015.03.080>

Copyright Elsevier

Additional Information

26 **ABSTRACT**

27 Bilayer films consisting of one layer of PCL with either one of thermoplastic starch (S)
28 or one of thermoplastic starch with 5 % PCL (S95) were obtained by compression
29 molding. Before compression, aqueous solutions of ascorbic acid or potassium sorbate
30 were sprayed onto the S or S95 layers in order to plasticize them and favour layer
31 adhesion. S95 films formed bilayers with PCL with very good adhesion and good
32 mechanical performance, especially when potassium sorbate was added at the interface.
33 All bilayers showed excellent barrier properties to water vapour and oxygen. Bilayers
34 consisting of PCL and starch containing 5% PCL, with potassium sorbate at the
35 interface, showed the best mechanical and barrier properties and interfacial adhesion
36 while having active properties, associated with the antimicrobial action of potassium
37 sorbate.

38

39 **Keywords:** starch, polycaprolactone, compression molding, interface, bilayer.

40

41 1. INTRODUCTION

42 In the last few years, the need for replacing petroleum-based plastics by biodegradable
43 polymers has led to a great number of studies focused on the design of environmentally
44 friendly materials. In particular, starch and its derivatives have been widely studied
45 since they could offer an inexpensive solution to such problems (Bastioli, 2001). Starch
46 is obtained from renewable resources, is widely available and low cost and it can be
47 used to obtain biodegradable films for food applications, as it has the ability to form
48 films or coatings with very low oxygen permeability (Zhang, Rempel & McLaren,
49 2014; Jiménez *et al.*, 2012). However, starch-based materials show several
50 disadvantages which reduce their applicability as packaging material, such as their
51 highly hydrophilic character, limited mechanical properties and the retrogradation
52 phenomena that occur during ageing. The blending of starch with other, more
53 hydrophobic, polymers is a widely studied strategy used to improve properties of starch
54 films. The aliphatic polyesters, such as polycaprolactone (PCL) or polylactic acid
55 (PLA), are synthetic biodegradable materials of a more hydrophobic nature that can be
56 combined with starch in different ways to modulate the properties of mixed films. Of
57 them, PCL has the advantage of great stretchability and low water vapour permeability
58 (Averous, Moro, Dole & Fringant, 2000). Nevertheless, the starch-PCL materials
59 obtained by simple blending are not adequate due to the low affinity of both polymers,
60 which leads to polymer phase separation with limited adhesion between the polymer
61 interfaces, thus resulting in poor film properties (Avella, Errico, Laurienzo, Martuscelli,
62 Raimo & Rimedio, 2000). To overcome this, several authors have studied the
63 improvement in the starch-PCL compatibility by using different compounds, which can
64 increase the polymer affinity via different mechanisms, such as PCL-co-pyromellitic
65 anhydride (Avella *et al.*, 2000) methylenediphenyldiisocyanate (Wang, Sun & Seib,

66 2001) or dioctyl maleate (Zhang & Sun, 2004). Nevertheless, the use of these kinds of
67 compounds can compromise the use of films for food packaging due to their potential
68 toxicity. Other authors reported that hydrogen bonds can be established to a certain
69 extent between the starch hydroxyls and the PCL carbonyls at the interface region,
70 which could allow the incorporation of small amounts of PCL in starch matrices without
71 notable polymer separation, improving film properties (Matzinos *et al.*, 2002; Ortega-
72 Toro *et al.*, 2015a, b).

73 The development of multilayer films using starch and PCL layers could be a good
74 alternative for developing packaging materials for food applications. A multilayer
75 packaging material can be defined as two or more materials with specific properties
76 combined in a single layered structure. The multilayer films with petrochemical-based
77 materials are already widely used in food packaging applications. (Fang, Fowler, Escrig,
78 Gonzalez, Costa & Chamudis, 2005; Mensitieri, Di Maio, Buonocore, Nedi, Oliviero,
79 Sansone & Iannace, 2011). The PCL-starch multilayers could exhibit some advantages,
80 such as the decrease in the overall moisture sensitivity and the improvement in the
81 mechanical properties (Yu, Dean & Bi, 2006), by combining the properties of each
82 material (Fabra, Busolo, Lopez-Rubio & Lagaron, 2013). Therefore, starch-PCL
83 multilayers could maintain the excellent gas barrier properties of the starch and the high
84 water vapour barrier of the PCL, which would be difficult to achieve with a single
85 biopolymer-based material. Layered structures based on biopolymers containing
86 antimicrobial compounds have been obtained by co-extrusion (Alix, Mahieu, Terrie,
87 Soulestin, Gerault, Feuilloley, Gattin, Edon, Ait-Younes & Leblanc, 2013) or
88 compression-molding (Takala, Salmieri, Boumail, Khan, Dang, Chauve, Bouchard &
89 Lacroix, 2013).

90 The incorporation of antioxidant and antimicrobial agents in biodegradable films has
91 been widely studied to obtain active packaging materials with controlled release of
92 bioactives (Ayranci & Tunc, 2003; Wook *et al.* 2013) to enhance food stability and
93 shelf life. These agents have often been included in the biopolymer dispersions used for
94 casting films (Gómez-Guillén, Ihl, Bifani, Silva & Montero, 2007; Jiménez, Fabra,
95 Talens & Chiralt, 2013; Cian, Salgado, Drago, González & Mauri, 2014). Nevertheless,
96 the usual thermal processing of bioplastics make their incorporation necessary during
97 the extrusion or other hot melting steps used at industrial level. Some losses of active
98 compounds can occur during this step due their thermosensitive. For instance, Wook *et*
99 *al* (2013) reported losses of resveratrol and α -tocopherol incorporated in PLA/starch
100 blend films during the polymer melt blending, ranging between 4 and 26 %, depending
101 on the film formulation.

102 The aim of this work is to analyse the properties of starch-PCL bilayer films obtained
103 by compression molding by incorporating a common food antimicrobial (potassium
104 sorbate: PS) and an antioxidant (ascorbic acid: AA) at the layers' interface. The
105 interactions of these compounds with both phases could improve the layers' adhesion,
106 while conferring active properties to the layered film. Bilayer films formed with starch
107 layers containing 5 % PCL was compared with those formed with pure starch layers in
108 order to discover the potential improvement of starch-PCL interfacial adhesion when a
109 small amount of PCL is present in the starch matrix.

110

111 **2. MATERIALS AND METHODS**

112 **2.1 Materials**

113 Corn starch was purchased from Roquette (Roquette Laisa España, Benifaió, Spain). Its
114 moisture content was 10 % w/w and amylose percentage was 14%. Glycerol was from

115 Panreac Química, S.A. (Castellar del Vallès, Barcelona, Spain). Polycaprolactone (PCL)
116 was from Aldrich Chemistry (Sigma-Aldrich Co. LLC Madrid, Spain), with a molecular
117 weight of 80.000 daltons. Potassium sorbate, ascorbic acid, magnesium nitrate 6-
118 hydrate, sodium chloride and phosphorus pentoxide were from Panreac Química, S.A.
119 (Castellar del Vallés, Barcelona, España).

120

121 **2.2 Film preparation**

122 Three kinds of monolayer films were obtained by melt blending and subsequent
123 compression molding: thermoplastic starch (S), thermoplastic starch with 5 % (g/100g
124 of starch) PCL (S95) and pure PCL (PCL). To prepare S films, native starch and
125 glycerol were dispersed in water using a starch:glycerol ratio of 1:0.3 w/w. When starch
126 films contained PCL, this was added to aqueous dispersions in 1:0.05, w/w starch:PCL
127 ratio.

128 A two-roll mill (Model LRM-M-100, Labtech Engineering, Thailand) was used for the
129 hot-mixing process where polymers were heated at 160 °C and 8 rpm for 30 min. The
130 resulting sheets were ground and conditioned at 25 °C and 75% RH using NaCl
131 oversaturated solutions for 48 h. Afterwards, the monolayer films were obtained using a
132 compression molding press (Model LP20, Labtech Engineering, Thailand). The
133 following process conditions were used: a) pre-heating cycle at 160 °C for 5 min, b)
134 compression-molding at 50 bar for 2 min, c) compression-molding at 150 bar for 6 min,
135 and d) cooling cycle at 150 bars for 3 min.

136 Subsequently, the bilayer films were obtained by means of a second compression-
137 molding step where the corresponding two layers were compressed together. The
138 process conditions were 80 °C and 150 bars for 4 min and cooling cycle for 2 min. The
139 obtained bilayer films always had one PCL layer and an S or S95 layer. Before the

140 second compression, 1 mL of distilled water (H₂O) or aqueous solutions containing
141 ascorbic acid (AA) or potassium sorbate (PS) were sprayed onto the S or S95 layers in
142 order to plasticize starch and promote layer adhesion. The obtained bilayer films were
143 coded by indicating if the starch layer was S or S95 and the kind of solution sprayed
144 onto the interface (H₂O, AA or PS); e.g. S-H₂O indicates that the bilayer film contains
145 S plus PCL layers sprayed with pure water. AA and PS aqueous solutions were prepared
146 in such a way that 1 mL of solution contained 0.1 g of compound /g of starch film. The
147 bilayer films were conditioned at 25 °C and 53% RH for 1 and 5 weeks before their
148 characterization. The thickness of conditioned films was measured at six random
149 positions with a digital electronic micrometer (Palmer-Comecta, Spain, ± 0.001 mm).

150

151

152 **2.3 Film characterization**

153 2.3.1 Scanning Electron Microscopy (SEM)

154 Cross-section images from resulting films were obtained by means of a scanning
155 electronic microscope (JEOL, JSM-5410, Japan). The conditioned samples (1 and 5
156 weeks) were stored inside P₂O₅ desiccators for one week before the analysis.
157 Afterwards, the samples were cryofractured, fixed on copper stubs, gold coated, and
158 observed using an accelerating voltage of 10 kV.

159

160 2.3.2 Fourier Transform Infrared (FTIR) spectroscopy

161 Attenuated Total Reflection Fourier Transform Infrared (ATR-FTIR) spectroscopy was
162 used to analyse component interactions in the films. Measurements were performed at
163 25 °C using a Tensor 27 mid-FTIR Bruker spectrometer (Bruker, Karlsruhe, Germany)
164 attached to a platinum ATR optical cell and an RT-D1a TGS detector (Bruker,

165 Karlsruhe, Germany). The diaphragm was set at 4 mm for the analysis, and the spectra
166 were obtained between 4,000 and 800 cm^{-1} using a resolution of 4 cm^{-1} . The analysis
167 was carried out on both the S or S95 and PCL layers. The data were analyzed using
168 OPUS software (Bruker, Karlsruhe, Germany).

169

170 2.3.3 Thermal properties

171 Thermal degradation of the films and their components was analysed using a
172 thermogravimetric TGA 1 Star^e System analyser (Mettler-Toledo, Inc., Switzerland),
173 equipped with an ultra-micro weighing scale ($\pm 0.1 \mu\text{g}$), under nitrogen atmosphere. The
174 analysis was carried out using the following temperature programme: heating from 25
175 to 500 $^{\circ}\text{C}$ at a 10 $^{\circ}\text{C}/\text{min}$ heating rate. Approximately 4 mg of each sample were used in
176 each test, considering at least two replicates for each one. Initial degradation
177 temperature (Onset) and peak temperature (Peak) were registered from the first
178 derivative of the resulting weight loss curves.

179

180 2.3.4 Water content (X_w)

181 Conditioned films were transferred to a natural convection oven (J.P. Selecta, S.A.,
182 Barcelona, Spain) at 60 $^{\circ}\text{C}$ for 24 h. Then, these samples were stored in a P_2O_5
183 desiccator for 8 days. Moisture content in dry basis was obtained from the initial and
184 final sample weights.

185

186 2.3.5 Film solubility in water

187 Pieces of dry samples were transferred to glass pots, and covered with bidistilled water
188 at a film:water ratio of 1:9 w/w. After 48 h, the samples were transferred to a natural
189 convection oven at 60 $^{\circ}\text{C}$ for 24 h in order to remove the water contained in bilayer

190 films. Finally, the samples were stored in a desiccator containing P₂O₅ for 8 days to
191 complete drying. Film water solubility was estimated from its initial and final weights.
192 Three replicates were considered per formulation.

193

194 2.3.6 Water Vapour Permeability (WVP)

195 The Water Vapour Permeability (WVP) of films was determined according to a
196 modification of E96-95 gravimetric method (ASTM, 1995) proposed by *McHugh et al.*
197 (1993). The measures were carried out exposing the S or S95 layer to 100% RH. To this
198 end, 5 mL of bidistilled water were placed in Payne permeability cups (3.5 cm diameter,
199 Elcometer SPRL, Hermelle/s Argenteau, Belgium). These cups were transferred to a
200 desiccator containing oversaturated Mg(NO₃)₂ (53% RH) at 25 °C. The permeability
201 measurements were performed by weighing the cups periodically (every 1.5 h for 24 h).
202 Eq. (1) proposed by *McHugh et al. (1993)* was used to calculate the vapour pressure on
203 the film's inner surface (p₂).

204

$$205 \quad WVTR = \frac{P \cdot D \cdot L_n [P - p_2 \setminus P - p_1]}{R \cdot T \cdot \Delta z} \quad (1)$$

206

207 where P, total pressure (atm); D, diffusivity of water through air at 25 °C (m²/s); R, gas
208 law constant (82.057 × 10⁻³ m³ atm kmol⁻¹ K⁻¹); T, absolute temperature (K); Δz, mean
209 stagnantair gap height (m), considering the initial and final z value; p₁, water vapour
210 pressure on the solution surface (atm); and p₂, corrected water vapour pressure on the
211 film's inner surface (atm). Water vapour permeance was calculated using Eq. (2) as a
212 function of p₂ and p₃ (pressure on the film's outer surface in the cabinet). Multiplication
213 of permeance by film thickness leads to the WVP of films.

214

215 $permeance = \frac{WVTR}{p_2 - p_3}$ (2)

216

217 In a first approach, the WVP of S-H₂O and S95-H₂O bilayer films was determined by
218 exposing PCL layer to both the 100% and 53% RH atmospheres in order to verify if
219 there were significant differences among WVP values. As none were observed,
220 measurements were carried out by exposing the starch layer (S or S95) to 100% RH in
221 every case. Values were obtained in triplicate for each film.

222

223 2.3.7 Oxygen Permeability (OP)

224 The oxygen permeability (OP) was determined using an Oxtran 1/50 (Mocon,
225 Minneapolis, USA) system considering the Standard Method [D3985-95 \(ASTM, 2002\)](#)
226 at 25 °C and 53 % RH. Three films were evaluated for each formulation. The assay was
227 performed exposing the PCL layer to the highest oxygen concentration in every case.
228 The transmission values were determined every 20 min until equilibrium was reached.
229 The exposure area during the tests was 50 cm² for each sample. To obtain the oxygen
230 permeability, the film thickness was considered.

231

232 2.3.8 Tensile properties

233 A universal test Machine (TA.XTplus model, Stable Micro Systems, Haslemere,
234 England) was used to determine the elastic modulus (EM) and tensile strength (TS) and
235 elongation (E) at break point of the films, following [ASTM standard method D882](#)
236 [\(ASTM, 2001\)](#). Films conditioned at 25 °C and 53% RH for 1 and 5 weeks were
237 evaluated. EM, TS, and E were determined from the stress-strain curves, estimated from
238 force-distance data obtained for the different films (2.5 cm wide and 5 cm long).

239 Samples were mounted in the film-extension grips of the testing machine and stretched
240 at 50 mm min⁻¹ until breaking. At least ten replicates were obtained from each sample.

241

242 2.3.9 Optical properties

243 The films' surface gloss was determined by means of a surface gloss meter (Multi Gloss
244 268, Minolta, Germany) at 85° incidence angle, since films exhibit low gloss, according
245 to **D523 standard method (ASTM, 1999)**. Each film was measured in triplicate on both
246 film faces. Results were expressed as gloss units (GU), relative to a highly polished
247 surface of black glass standard with a value near to 100 GU.

248 Film transparency was determined from the surface reflectance spectra (400 – 700 nm)
249 obtained by a Minolta spectro-colorimeter (CM-3600d model, Minolta Co., Tokyo,
250 Japan) on both white and black backgrounds. Kubelka-Munk theory for multiple
251 scattering was applied in order to determine the internal transmittance (Ti). The Ti of
252 the films was determined using eq. (3). In this equation, R₀ is the reflectance of the film
253 on an ideal black background. Parameters *a* and *b* were calculated by means of eqs. (4)
254 and (5), where R is the reflectance of the sample backed by a known reflectance, R_g.

255

$$256 \quad T_i = \sqrt{(a - R_0)^2 - b^2} \quad (3)$$

257

$$258 \quad a = \frac{1}{2} \left(R + \frac{R_0 - R + R_g}{R_0 R_g} \right) \quad (4)$$

259

$$260 \quad b = \sqrt{a^2 - 1} \quad (5)$$

261

262 2.3.10. Statistical analysis

263 Statgraphics Plus for Windows 5.1 (Manugistics Corp., Rockville, MD) was used to
264 carry out statistical analyses of data through an analysis of variance (ANOVA). Fisher's
265 least significant difference (LSD) was used at the 95% confidence level.

266

267 **3. RESULTS**

268 **3.1. Structural properties**

269 Figure 1A shows the micrographs of the cross section of some of the studied bilayer
270 films where the two polymer layers can be clearly distinguished. PCL layer was much
271 thinner than that of starch, despite the fact that films of similar weight were compressed
272 together. Table 1 shows the thickness values of the mono- and bilayers. S and S95
273 bilayers showed values close to those of the initial starch monolayer, which indicated
274 that both starch and PCL layers became thinner during the second compression.
275 However, SEM micrographs show that PCL films flow to a greater extent during the
276 second compression step, giving rise to PCL layers of about 30-50 μm , while the starch
277 layers barely decrease in their original thickness, especially the S95. This agrees with
278 the higher flowability of the more plastic PCL material. At the temperature of the
279 second compression (80°C), the melting temperature of PCL (63.5 °C, [Ortega-Toro et al. 2015a](#))
280 [al. 2015a](#)) was reached, while starch (Tg: 126 °C, [Ortega-Toro et al. 2015a](#)) was only
281 plasticized at surface level by the moisturising effect of the sprayed solution. The S95
282 bilayers were thicker which indicates that the presence of PCL in starch films decreased
283 their ability to flow during compression. This can be attributed to the reduced water
284 affinity of the starch phase when PCL was finely dispersed in the matrix, which inhibits
285 the water plasticization effect of the sprayed solution.

286 The interfacial adhesion of PCL and starch layers can be observed in Figure 2, where
287 the interface of the different bilayer films is clearly observed. Each layer shows its

288 typical fracture appearance; pure starch exhibits a continuous and homogeneous aspect,
289 whereas fine, well dispersed PCL particles can be observed in the S95 layer. Previous
290 studies (Ortega-Toro *et al.*, 2015a, b) demonstrated a small degree of miscibility of PCL
291 in starch, through the depression of the starch glass transition temperature when PCL
292 was added. PCL layers exhibit filamentous formations, associated with the plastic
293 fracture of their amorphous zones, in agreement with the very low PCL Tg (-61.5 °C,
294 Averous *et al.*, 2000). At higher magnification (Figure 1B), the penetration of fine
295 channels of the PCL phase (arrows) into the starch phase can be observed forming
296 union points between layers. This is probably favoured by the plasticization induced in
297 the starch layer surface by the aqueous solutions sprayed before the compression step.
298 When the starch layer contained PCL, the PCL which flows into the starch phase can
299 bond to the dispersed, melted PCL particles, thus contributing to the layer adhesion. In
300 Figure 2, greater layer adhesion can be observed in films containing S95, especially
301 when the surface was sprayed with potassium sorbate aqueous solution, where the
302 interface can barely be observed.

303 Figure 3 shows the infrared spectra obtained from the starch face and the wavenumber
304 corresponding to the most characteristic peaks of the compounds present in the different
305 formulations. Spectra obtained from the PCL layer did not differ from that of pure PCL
306 and they were not included. This could indicate that no significant diffusion of
307 compounds added at the interface (AA or PS) occurred through the PCL layer, although
308 they could act at interfacial level.

309 The spectra of the S95 films showed some differences with respect to those of pure
310 starch, showing characteristic peaks of both S and PCL, with some band shifts. The
311 carbonyl group band (C=O stretching) was shifted with respect to pure PCL, which

312 suggests the formation of hydrogen bonds between PCL carbonyl and starch hydroxyls,
313 as reported by other authors (Cai *et al.*, 2014).

314 Likewise, small shifts in some peaks can be detected for starch bilayers, as compared to
315 the corresponding bands of the S or S95 monolayer films. This suggests that some
316 changes in molecular interactions inside the starch matrix occurred, associated with the
317 diffusion of compounds added at the interface.

318 Shifts in bands corresponding to C-O-C ($1049\text{-}1153\text{ cm}^{-1}$), C=O ($1724\text{-}1728\text{ cm}^{-1}$) and –
319 OH ($3300\text{-}3319\text{ cm}^{-1}$) can be due to the presence of small amounts of AA or PS,
320 diffused together with water molecules inside the starch phase. The hydroxyl vibration
321 band showed the highest shift with respect to the S or S95 films, which can be due to
322 the higher hydration of the starch layer due to the surface wetting with the
323 corresponding solution.

324

325 **3.2. Thermal behaviour**

326 Thermogravimetric analysis allows us to obtain information about the effect of
327 compounds added at the interface on the thermal stability of polymers, due to their
328 diffusion into the layers and potential interactions with each macromolecule. Figure 4
329 shows the DGTA curves of the bilayers, showing the peaks associated with the different
330 weight losses caused by thermal degradation. All the curves showed three separate
331 steps: a) small, broad peak due to evaporation of bonded water between 50 and 100 °C;
332 b) starch thermal degradation between 283 °C and 290 °C and c) PCL thermal
333 degradation at about 374°C. Table 2 shows thermal degradation temperatures (onset and
334 peak) of mono- and bilayer films. The PCL addition to the starch (S95 sample) provoked
335 a significant increase ($p > 0.05$) in the starch degradation temperature (onset and peak)
336 while the onset temperature of PCL phase also rose. This indicates that polymer

337 interactions improved the thermal stability of both phases. In bilayers, degradation
338 temperatures of both starch and PCL increased (more in the case of starch), except when
339 PS was added. In these cases, the thermal degradation of polymers in bilayers occurred
340 at a lower temperature than in the corresponding monolayer. This indicates that PS
341 diffused from the interface inside the polymer matrices and the induced molecular
342 interactions with both polymers affected their thermal degradation behaviour. The
343 interactions of PS with polymer layers promoted layer adhesion, as deduced by SEM.
344 As a reference, the TGA of the glycerol, AA and PS was carried out. The onset
345 temperatures for each compound were 212 °C, 196 °C and 448 °C respectively, which
346 guarantees their stability at the temperatures used in the film thermoprocessing
347 (maximum 160°C). AA and PS were only heated up to 80 °C during the second
348 compression. So, the antioxidant effect of AA and the antimicrobial activity of PS could
349 be preserved after compression molding. In fact, the pure PS showed the highest
350 thermal stability, although it promoted the thermal degradation of starch and PCL.
351 Flores *et al.* 2010 also reported that the PS concentration in tapioca starch–glycerol
352 based edible films was not affected by the extrusion process and the preservative was
353 available to act as an antimicrobial agent.

354

355 **3.3. Physical properties**

356

357 In Table 1, the water content and film solubility in water are also shown for all the
358 samples conditioned at 25°C and 53% RH for 1 and 5 weeks. At the initial time, water
359 content of bilayers was higher than that of S or S95 films due to water absorption of the
360 sprayed solution and their slow equilibration with the external atmosphere (53% RH).

361 Nevertheless, after 5 storage weeks, every bilayer had a similar water content (6-8 %) in
362 the range of the starch (S or S95) films.

363 Water solubility of S95 bilayers showed homogenous values which did not change after
364 5 storage weeks, whereas S bilayers showed higher solubility after 1 one storage week,
365 when they have a high moisture content, but lower solubility at 5 storage weeks when
366 the film moisture content fell. In S95 bilayers, solubility was reduced to about half of
367 the corresponding value of the S layer, which is coherent with the very low water
368 solubility of the PCL layer. During the solubility test, S95 bilayers remained adhered,
369 whereas in S bilayers, separation occurred at the edges of the films.

370 Figure 5 shows typical Stress–Hencky Strain curves of the monolayer and bilayer films
371 after 1 week conditioned at 53%RH and 25°C. The S95 monolayer exhibited lower
372 stress values than the S layer, but greater extensibility. The addition of PCL to the starch
373 matrix provoked a twofold effect on the mechanical response of the film: matrix
374 plasticization effect (Tg decrease of starch) caused by the small PCL miscible fraction
375 and matrix discontinuity due to the non-compatible PCL fraction. Both effects caused
376 weakening of the cohesion forces of the starch phase which decreased the elastic
377 modulus and the tensile strength, although the plasticizing effect enhanced the film
378 stretchability. PCL is a ductile polymer with high deformability, whose deformation at
379 break is near 500 % ([Averous et al., 2000](#); [Matzinos et al., 2002](#)), which was not
380 reached during the tensile test.

381 The bilayer films did not exhibit a net break but they showed successive micro-fractures
382 from a determined deformation level till the total breakdown of the film. This can be
383 associated with the progressive detachment of the film layers during the tensile test till
384 total fracture. The value of the first fracture point was taken and shown in Table 3,
385 together with the elastic modulus and tensile strength at the first failure point.

386 Bilayer films showed slightly lower values of EM and TS than the S or PCL monolayer
387 but greater than the S95 monolayer, which indicates that the PCL layer reinforced the
388 S95 bilayer films. The incorporation of AA or PS into the interface slightly decreased
389 the EM values of bilayers, but significantly increased TS and deformation at break in
390 the S95 bilayers. The start of layer detachment (micro-fractures) takes place at a
391 deformation level of about 30 % in S95-AA and S95-PS bilayers, which indicates that
392 they were better adhered than in the other bilayer films when micro-fractures occurred
393 at lower deformation levels. In S bilayers, these compounds were not so effective at
394 promoting S-PCL adhesiveness. Therefore, the diffusion of AA and PS molecules to the
395 PCL chains near the interface in both PCL and S95 layers could promote stronger union
396 forces which contribute to the layer adhesion.

397 After 5 weeks of storage, all the films had higher EM values, especially S monolayers,
398 due to the phenomenon of starch retrogradation, which also reduced the film
399 extensibility. Nevertheless, S95 maintained a deformability level of about 40 % and the
400 S95-PS bilayer did not reduce its extensibility value. This bilayer exhibited the most
401 stable tensile behavior, which indicates that starch chain association was mitigated by
402 the combined effect of both PCL and PS interactions with starch chains. In general,
403 bilayers better maintain tensile properties throughout storage time. In fact, in no case
404 did tensile stress and deformation at break vary while EM increased in every case,
405 except for the S95-PS samples. The increase in EM can be caused by the reduction in
406 film water content shown in Table 1. The observed behavior suggests there were
407 positive interactions between layers inhibiting the changes in the starch phase, at least
408 near the PCL interface.

409 Table 4 shows the water vapour permeability (WVP) and the oxygen permeability (OP)
410 of the studied films conditioned at 25°C and 53% RH for 1 and 5 weeks. In general, the

411 WVP values of bilayers were very low, as compared with S or S95 monlayers, and
412 similar to the PCL monolayer. This was highly positive because an effective water
413 vapour barrier is very important in food packaging. The greater WVP of S95 than that
414 of the S monolayer can be explained by the plasticization effect of PCL in the starch
415 matrix, as commented on above (Ortega-Toro *et al.*, 2015b). After 5 weeks of storage,
416 no notable changes in the WVP values occurred; the bilayers maintained their high
417 water vapour barrier.

418 The oxygen permeability (OP) of starch films and bilayers was very low and in some
419 cases they were below the sensitivity threshold of the equipment. On the contrary, the
420 OP of PCL film reached the sensitivity limit. So, as expected, the barrier properties of
421 bilayers were greatly improved with respect to the starch or PCL films, exhibiting very
422 low OP (as starch) and WVP (as PCL). As regards the influence of adding AA or PS at
423 the interface, the most noticeable change was produced by PS, which reduces the OP in
424 both S and S95 bilayers to values lower than the detection limit of the Ox-Tran® used
425 to perform the test,. This coincides with the particular interactions of PS with S and
426 PCL, as deduced from the structural and thermal analysis.

427 Table 5 shows the gloss values at 85° of both faces of the films conditioned for 1 and 5
428 weeks. The gloss of S and S95 films was very similar and slightly lower than that of the
429 PCL. Likewise, the gloss of the starch and PCL faces in S bilayers was in the same
430 range as that of the respective controls (S and PCL): However, the S95 bilayers
431 presented lower gloss at both faces than the isolated S95 or PCL films. This is coherent
432 with the special role which dispersed PCL plays in S95 layers, that of favoring the layer
433 bonding. The PCL of both S95 and PCL layers melt at 80°C and this contributes to
434 compound interpenetration during the second compression, unifying itself after cooling.
435 This melting-crystallization process of PCL at both layers could generate both more

436 union points at the interface and micro-irregularities on each layer surface. This is a key
437 factor in the engineering design of starch-based bilayers, because it promotes the
438 material stability over time inhibiting the starch retrogradation, as deduced from
439 mechanical behavior after 5 storage weeks.

440 Figure 6 shows the spectral distribution curves of internal transmittance (T_i) of the films
441 conditioned at 25 °C and 53% RH for 1 week. The results obtained, considering both
442 starch or PCL faces as beam incidence surfaces, did not present significant differences.
443 So, the mean values were considered. In general, films with an isotropic structure have
444 high T_i values since no light dispersion occurs ([Villalobos *et al.*, 2005](#); [Ortega-Toro *et al.*, 2014](#)).
445 The S monolayer was the most transparent, whereas PCL showed a greater
446 opacity. The S95 monolayer lost transparency with respect to the pure starch film due to
447 the presence of a PCL dispersed phase which provoked light dispersion. Bilayers
448 showed transparency levels in the order of those of S95, but the S95 bilayers were
449 slightly more opaque due to the effect of dispersed PCL particles and non-isotropic
450 bilayer formation.

451

452 **4. CONCLUSIONS**

453 Bilayer films of thermoplastic corn starch and PCL could be obtained by compression
454 molding at 80°C, by moisturising the interface with aqueous solutions containing
455 ascorbic acid or potassium sorbate which, in turn, can confer active properties to the
456 films. Starch layers containing 5 % PCL formed bilayers which were very well adhered
457 with PCL and exhibited good mechanical performance, especially when potassium
458 sorbate was added at the interface. All the bilayers showed excellent water vapour and
459 oxygen permeability due to the association of two layers with very good barrier
460 properties to each one. Bilayers consisting of PCL and starch containing 5% PCL, with

461 potassium sorbate at the interface, had the best mechanical and barrier properties and
462 interfacial adhesion while also having active properties associated with the
463 antimicrobial action of potassium sorbate. A study of the release of this compound in
464 different food simulants is running in order to evaluate its potential in food preservation.

465

466 **ACKNOWLEDGEMENTS**

467 The authors acknowledge the financial support from the Spanish Ministerio de
468 Educación y Ciencia throughout the project AGL2013-42989-R. Rodrigo Ortega-Toro
469 thanks the Conselleria de Educació de la Comunitat Valenciana for the Santiago
470 Grisolíá grant. Authors also thank to Electron Microscopy Service of the UPV for their
471 technical assistance.

472

473 **REFERENCES**

- 474 Alix, S., Mahieu, A., Terrie, C., Soulestin, J., Gerault, E., Feuilloley, M.G.J., Gattin, R.,
475 Edon, V., Ait-Younes, T. & Leblanc, N. (2013). Active pseudo-multilayered films
476 from polycaprolactone and starch based matrix for food-packaging applications.
477 *European Polymer Journal*, 49: 1234 – 1242.
- 478 Avella, M., Errico, M.E., Laurienzo, P., Martuscelli, E., Raimo, M. & Rimedio, R.
479 (2000). Preparation and characterization of compatibilised polycaprolactone/starch
480 composites. *Polymer*, 41: 3875 – 3881.
- 481 ASTM. 1995. Standard test methods for water vapour transmission of materials.
482 Standard Designations: E96-95. Annual book of ASTM standards Philadelphia, PA:
483 American Society for Testing and Materials.

484 ASTM. 1999. Standard test method for specular gloss. Standard Designations: D523. In
485 Annual book of ASTM standards, Philadelphia, PA: American Society for Testing
486 and Materials.

487 ASTM. 2001. Standard test method for tensile properties of thin plastic sheeting.
488 Standard Designations: D882. Annual book of ASTM standards. Philadelphia, PA:
489 American Society for Testing and Materials.

490 ASTM, 2002. Standard test method for oxygen gas transmission rate through plastic film
491 and sheeting using a coulometric sensor. Standard Designations: 3985-95. Annual
492 book of ASTM standards. Philadelphia, PA: American Society for Testing and
493 Materials.

494 Averous, L., Moro, L., Dole, P., & Fringant, C. (2000). Properties of thermoplastic
495 blends: starch polycaprolactone. *Polymer*, 41 (11): 4157-4167.

496 Ayranci, E. & Tunc, S. (2003). A method for the measurement of the oxygen
497 permeability and the development of edible films to reduce the rate of oxidative
498 reactions in fresh foods. *Food Chemistry*, 80: 423 – 431.

499 Bastioli, C. (2001). Global status of the production of biobased packaging materials.
500 *Starch/Stärke*, 53: 351-355.

501 Cai, J., Xiong, Z., Zhou, M., Tan, J., Zeng, F., Ma, M., Lin, S., & Xiong, H. (2014).
502 Thermal properties and crystallization behavior of thermoplasticstarch/poly(ϵ -
503 caprolactone) composites. *Carbohydrate Polymers*, 102: 746–754.

504 Cian, R.E., Salgado, P.R., Drago, S.R., González, R.J., Mauri, A.N. (2014).
505 Development of naturally activated edible films with antioxidant properties prepared
506 from red seaweed *Porphyra columbina* biopolymers. *Food Chemistry*, 146: 6 – 14.

507 Fabra, M.J., Busolo, M.A., Lopez-Rubio, A. & Lagaron, J.M. (2013). Nanostructured
508 bilayers in food packaging. *Trends in Food Science & Technology*, 31: 79 – 87.

509 Fang, J.M., Fowler, P.A., Escrig, C., Gonzalez, R., Costa, J.A. & Chamudis, L. (2005).
510 Development of biodegradable laminate films derived from naturally occurring
511 carbohydrate polymers. *Carbohydrate Polymers*, 60: 39 – 42.

512 Flores, S. K., Costa, D., Yamashita, F., Gerschenson, L. N., & Grossmann, M. V.
513 (2010). Mixture design for evaluation of potassium sorbate and xanthan gum effect
514 on properties of tapioca starch films obtained by extrusion. *Materials Science and*
515 *Engineering C*, 30:196–202.

516 Gómez-Guillén, M.C., Ihl, M., Bifani, V., Silva, A. & Montero, P. (2007). Edible films
517 made from tuna-fish gelatin with antioxidant extracts of two different murta ecotypes
518 leaves (*Ugni molinae* Turcz). *Food Hydrocolloids*, 21 (7): 1133 – 1143.

519 Jiménez, A., Fabra, M.J., Talens, P. & Chiralt, A. (2012). Edible and Biodegradable
520 Starch Films: A Review. *Food Bioprocessing Technology*, 5: 2058 – 2076.

521 Jiménez, A., Fabra, M.J., Talens, P. & Chiralt, A. (2013). Physical properties and
522 antioxidant capacity of starch–sodium caseinate films containing lipids. *Journal of*
523 *Food Engineering*, 116 (3): 695 – 702.

524 Matzinos, P., Tserki, V., Kontoyiannis, A. & Panayiotou, C. (2002). Processing and
525 characterization of starch/polycaprolactone products. *Polymer Degradation and*
526 *Stability*, 77: 17 – 24.

527 McHugh, T.H., Avena-Bustillos, R., & Krochta, J.M. (1993). Hydrophilic edible films-
528 Modified procedure for water-vapor permeability and explanation of thickness
529 effects. *Journal of Food Science*, 58 (4): 899–903.

530 Mensitieri, G., Di Maio, E., Buonocuore, G.G., Nedi, I., Oliviero, M., Sansone, L. &
531 Iannace, S. (2011). Processing and shelf life issues of selected food packaging
532 materials and structures from renewable resources. *Trends in Food Science and*
533 *Technology*, 22: 72 – 80.

534 Ortega-Toro, R., Jiménez, A., Talens, P., & Chiralt, A. (2014). Properties of starch-
535 hydroxypropyl methylcellulose based films obtained by compression molding.
536 Carbohydrate Polymers, 109 (30): 155–165.

537 Ortega-Toro, R., Collazo-Bigliardi, S., Talens, P., & Chiralt, A. (2015a). Influence of
538 citric acid on the properties and stability of starch-polycaprolactone based films (In
539 review) **Poner revista**

540 ~~Ortega-Toro, R., Muñoz, M.A., Talens, P., & Chiralt, A. (2015b). Starch based films~~
541 ~~obtained by compression molding: Effect of low proportion of polycaprolactone~~
542 ~~and/or polyethylene glycol. **Under submission.**~~

543 Takala, P.N., Salmieri, S., Boumail, A., Khan, R.A., Dang Vu, K., Chauve, G.,
544 Bouchard, J. & Lacroix, M. (2013). Antimicrobial effect and physicochemical
545 properties of bioactive trilayer polycaprolactone/methylcellulose-based films on the
546 growth of foodborne pathogens and total microbiota in fresh broccoli. *Journal of*
547 *Food Engineering*, 116: 648 – 655.

548 Villalobos, R., Chanona, J., Hernández, P., Gutiérrez, G. & Chiralt, A. (2005). Gloss and
549 transparency of hydroxypropyl methylcellulose films containing surfactants as
550 affected by their microstructure. *Food Hydrocolloids*, 19 (1): 53 – 61.

551 Wang, H., Sun, X. & Seib, P. (2001). Strengthening blends of poly(lactic acid) and
552 starch with methylenediphenyl diisocyanate. *Journal of Applied Polymer Science*,
553 82: 1761 – 1767.

554 Wook, S., Kie, J., Selke, S., Soto-Valdez, H., Matuana, L., Rubino, M. & Auras, R.
555 (2013). Migration of α -tocopherol and resveratrol from poly(L-lactid acid)/starch
556 blends films into ethanol. *Journal of Food Engineering*, 116: 814 – 828.

557 Yu, L., Dean, K. & Bi, L. (2006). Polymer blends and composites from renewable
558 resources. *Progress in Polymer Science*, 31: 576 – 602.

559 Zhang, J.F. & Sun, X. (2004). Mechanical and Thermal Properties of Poly(lactic
560 acid)/Starch Blends with Dioctyl Maleate. *Journal of Applied Polymer Science*, 94:
561 1697 – 1704.

562 Zhang, Y., Rempel, C. & McLaren, R. (2014). Chapter 16 - Thermoplastic Starch.
563 *Innovations in Food Packaging (Second Edition)*, 391 – 412.

564

565

566

567

568

569

570

571

572

573

574

575

576

577

578

579

580

581

582

583

584

585

586

587

588 Figure captions

589 Figure 1.- SEM micrographs of the cross section of some bilayer films, at low (A) and high magnification
590 levels (B) showing the layer interface.

591 Figure 2.- SEM micrographs of the cross section of the different bilayer films, showing the layer
592 interface.

593 Figure 3.- FT-IR spectra of monolayers (S, S95 and PCL) and starch-PCL bilayers (S-H₂O, S-AA, S-SP,
594 S95-H₂O, S95-AA, S95-SP) obtained from the starch face.

595 Figure 4. - DTGA curves of bilayer films showing peaks for starch degradation and PCL degradation.

596 Figure 5. - Typical stress–Hencky strain curves of the different films conditioned at 25 °C and 53%
597 relative humidity for 1 week.

598 Figure 6.- Spectral distribution curves of internal transmittance (Ti) of the studied films conditioned at 25
599 °C and 53% RH for 1 week.

600

601

602

603

604

605

606

607

608

609

610

611

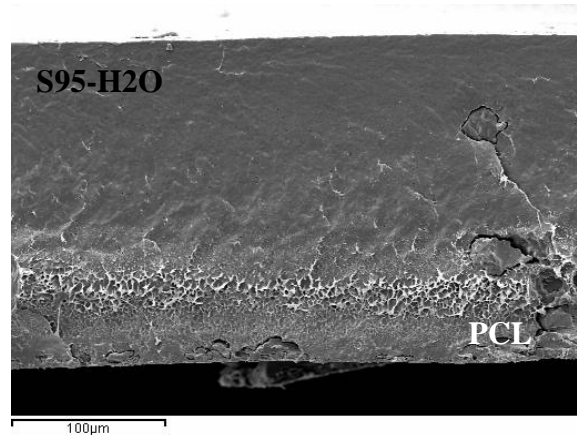
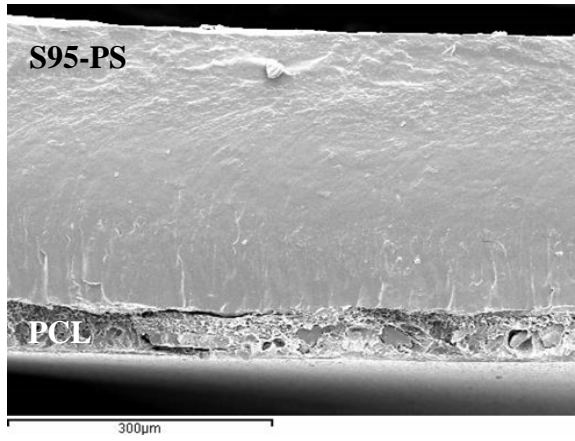
612

613

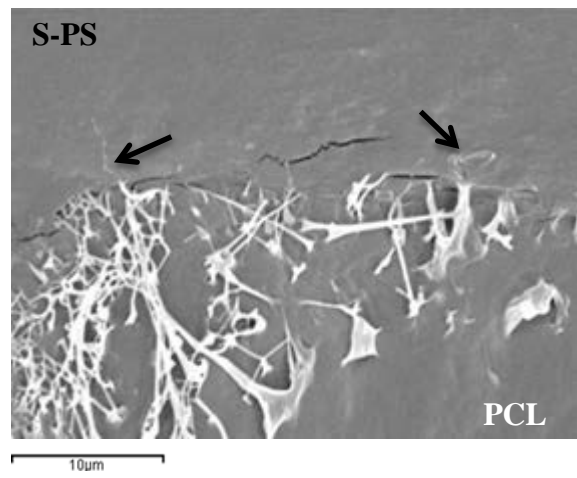
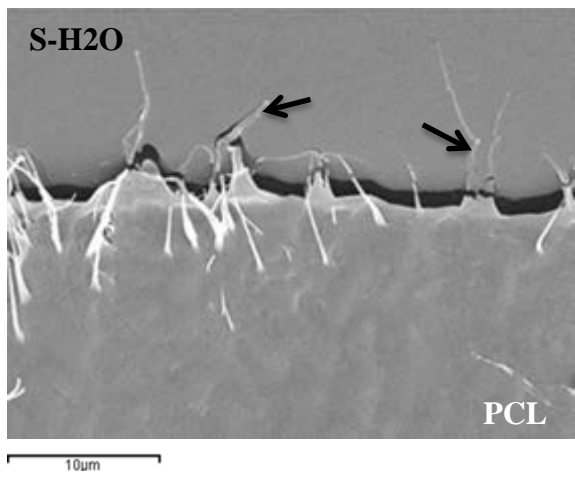
614

615

616



B



617

618 Figure 1

619

620

621

622

623

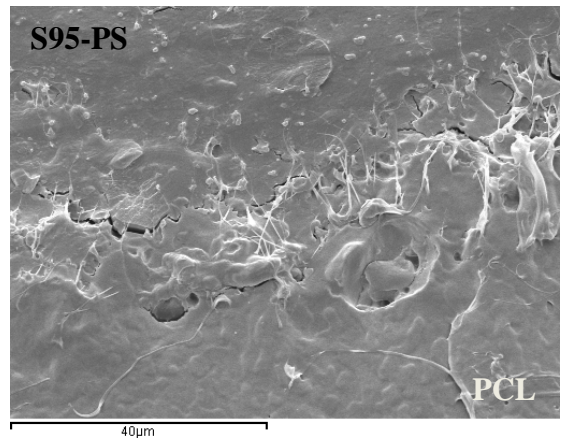
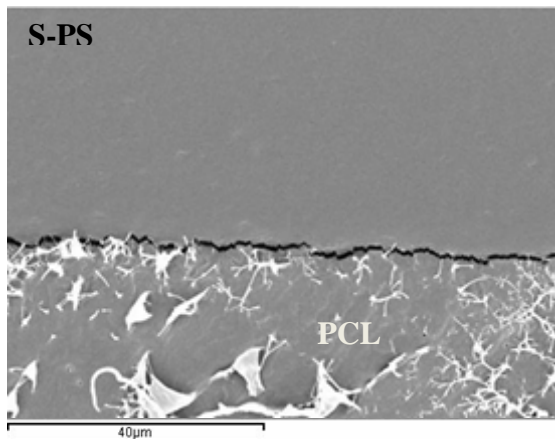
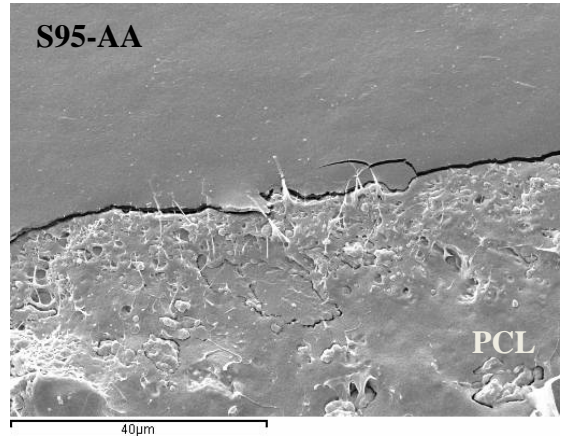
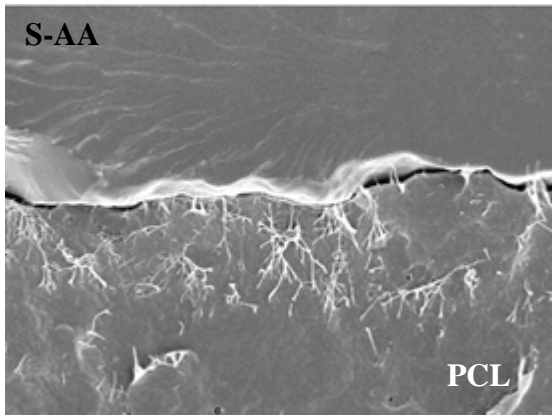
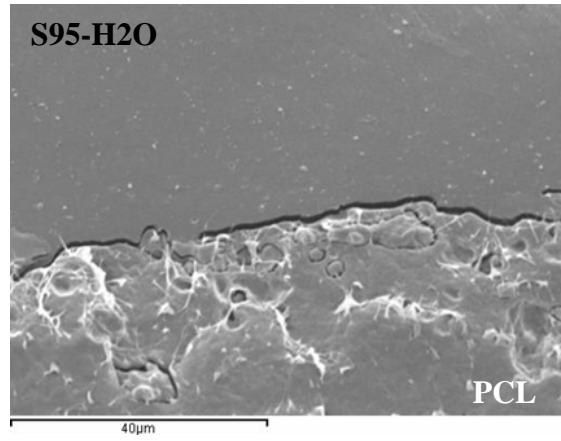
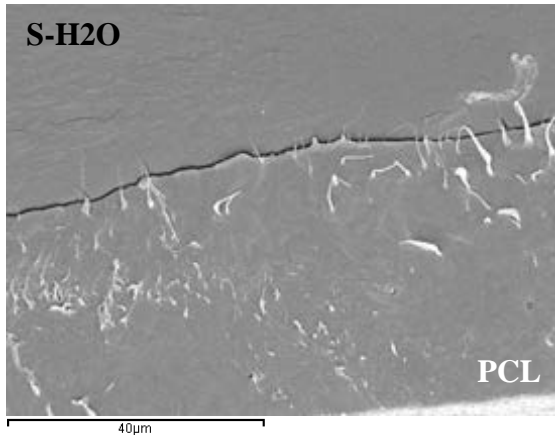
624

625

626

627

628



629

630 Figure 2

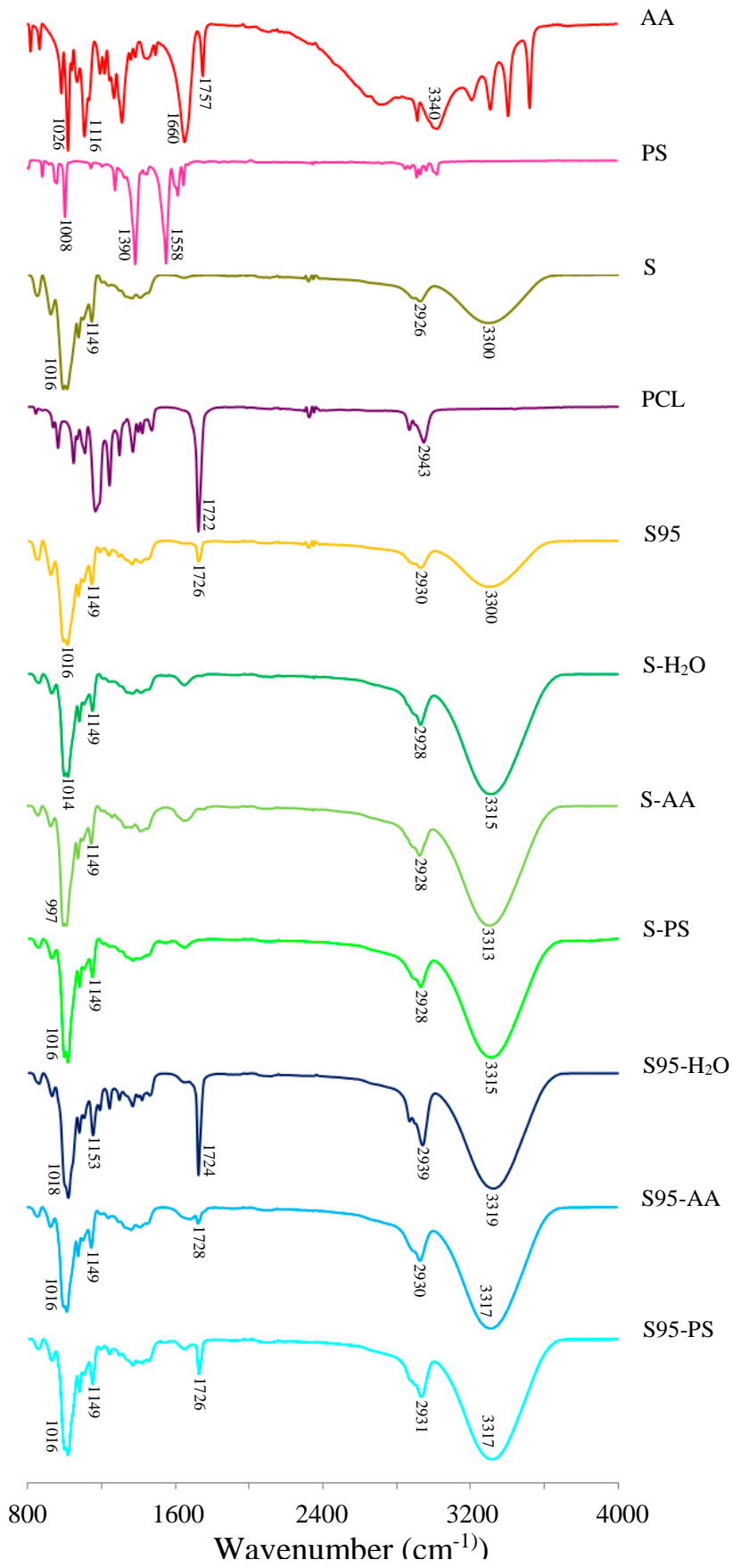
631

632

633

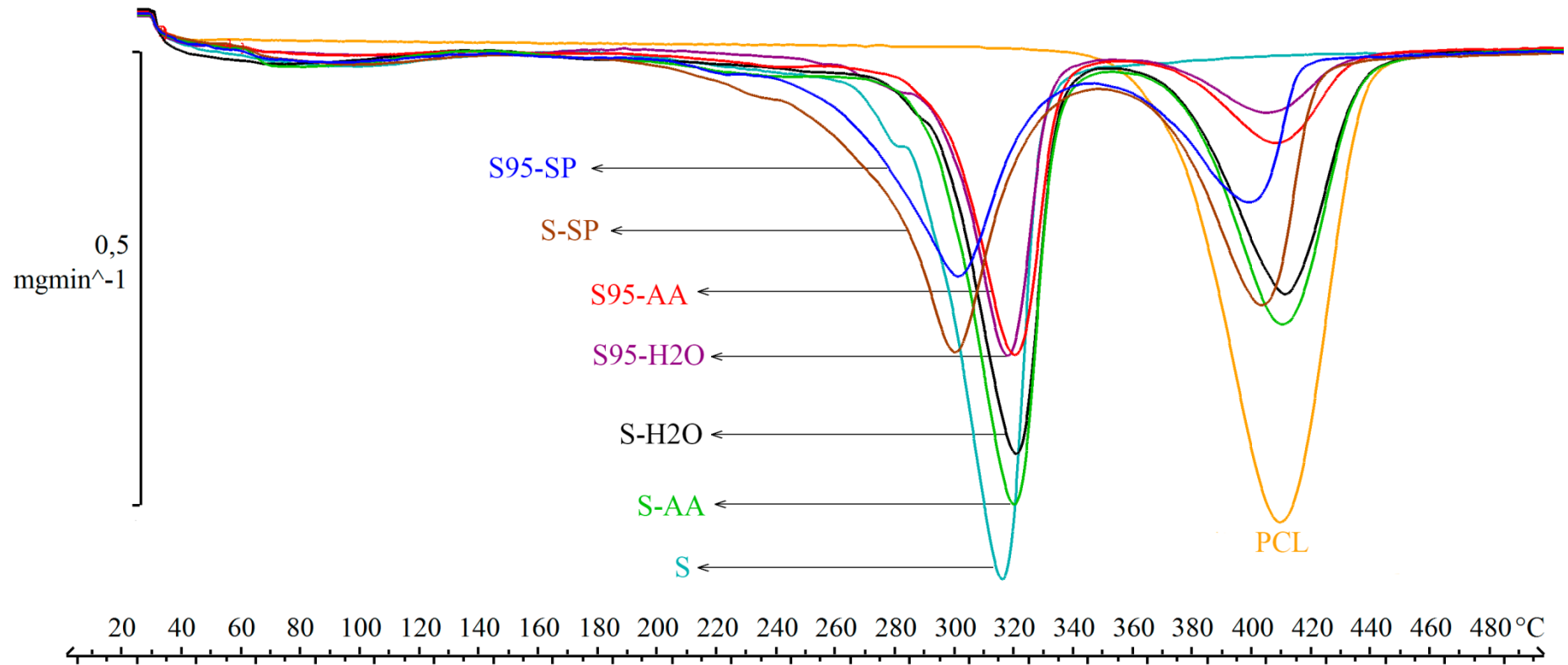
634

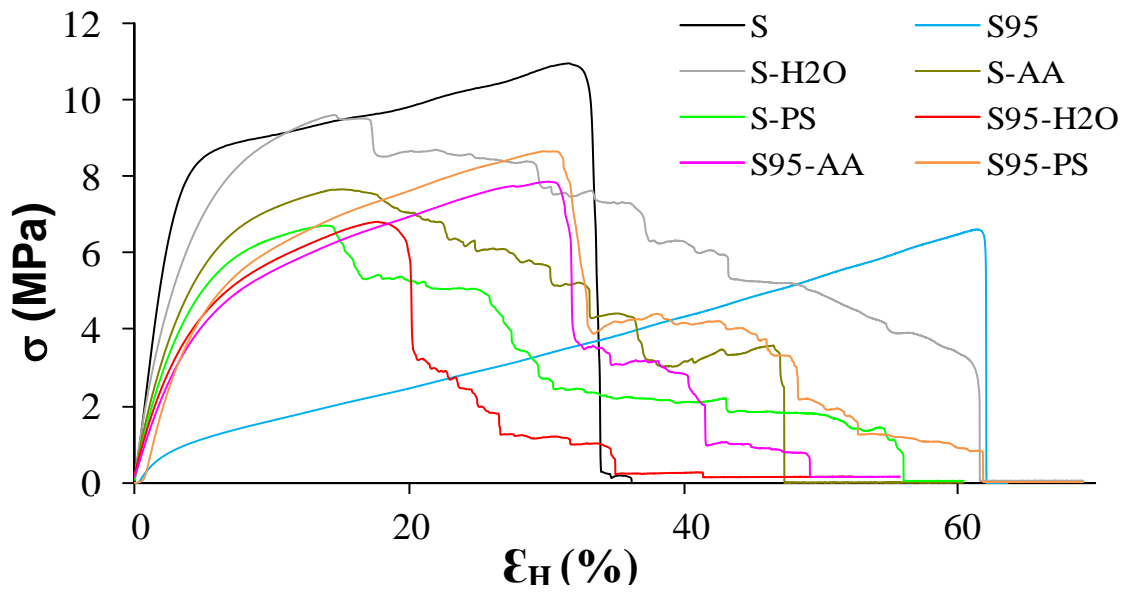
635



636

637 Figure 3.





642

643 Figure 5.

644

645

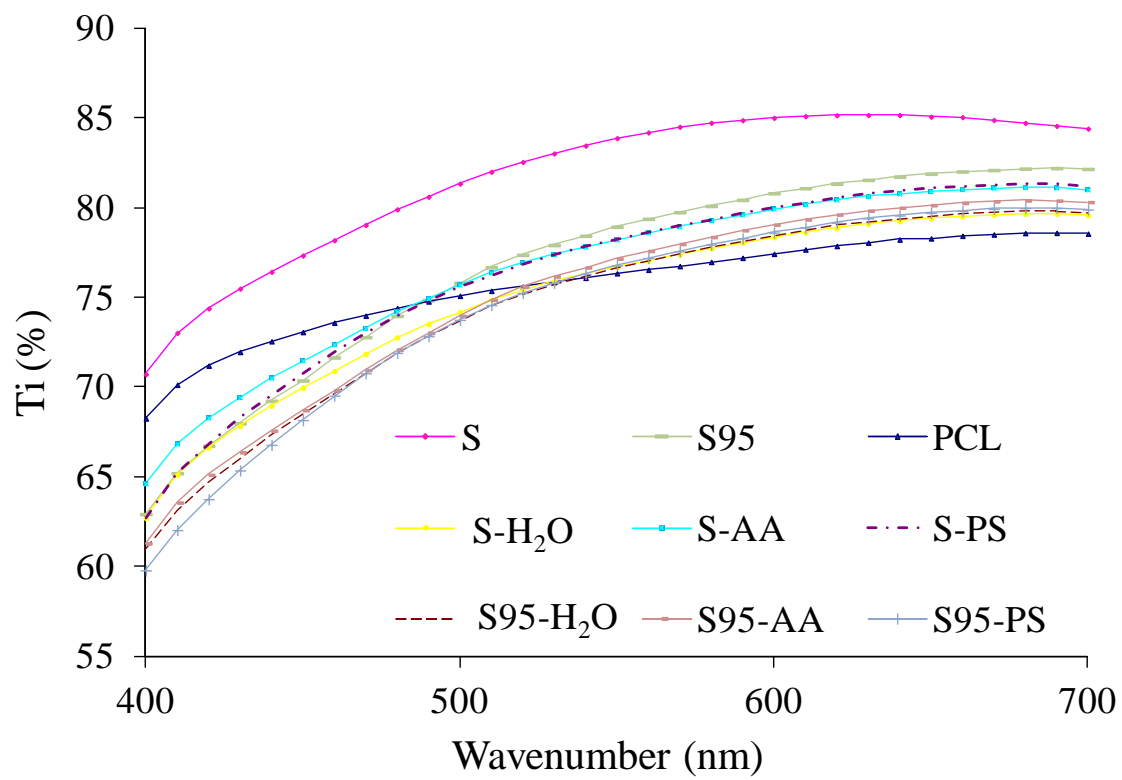
646

647

648

649

650



651

652 Figure 6.

653

654 Table 1. -Mean values and standard deviation of thickness, water content (g water/g dried film) and water solubility (g solubilised film/g initial dried film) of the different
 655 films stored at 53% relative humidity and 25 °C.

Films	Thickness (μm)	X_w		Film solubility	
		1 week	5 week	1 week	5 week
S	261 ± 22^{bc}	0.061 ± 0.006^{b1}	0.079 ± 0.004^{d2}	0.19 ± 0.07^{d1}	0.24 ± 0.05^{d1}
S95	268 ± 13^{bc}	0.091 ± 0.007^{c1}	0.1146 ± 0.0013^{e2}	0.18 ± 0.05^{cd1}	0.198 ± 0.004^{c1}
PCL	149 ± 17^a	0.003 ± 0.002^{a1}	0.0021 ± 0.0005^{a1}	0.00022 ± 0.00011^{a1}	0.0004 ± 0.0002^{a1}
S-H ₂ O	228 ± 7^b	0.372 ± 0.015^{g1}	0.060 ± 0.002^{bc2}	0.30 ± 0.02^{e1}	0.21 ± 0.04^{cd2}
S-AA	236 ± 2^b	0.25 ± 0.02^{f1}	0.058 ± 0.008^{b2}	0.20 ± 0.05^{d1}	0.114 ± 0.010^{b2}
S-PS	234 ± 5^b	0.46 ± 0.04^{h1}	0.066 ± 0.004^{c2}	0.38 ± 0.05^{f1}	0.297 ± 0.014^{e2}
S95-H ₂ O	283 ± 30^c	0.20 ± 0.02^{d1}	0.067 ± 0.008^{c2}	0.114 ± 0.009^{b1}	0.107 ± 0.014^{b1}
S95-AA	322 ± 25^d	0.220 ± 0.012^{de1}	0.085 ± 0.002^{d2}	0.123 ± 0.012^{bc1}	0.142 ± 0.016^{b1}
S95-PS	325 ± 14^d	0.237 ± 0.011^{ef1}	0.0804 ± 0.0015^{d2}	0.123 ± 0.017^{bc1}	0.120 ± 0.013^{b1}

656
 657 Different superscript letters within the same column indicate significant differences among formulations ($p < 0.05$).

658 Different superscript numbers within the same row indicate significant differences due to storage time ($p < 0.05$).

659

660

661

662

663

664

665 Table 2.- Mean values and standard deviation of thermal degradation of starch and PCL of the studied bilayers equilibrated at 53% relative humidity and 25 °C

Films	Starch		PCL	
	Onset (°C)	Peak (°C)	Onset (°C)	Peak (°C)
S	283 ± 7 ^c	313.8 ± 0.4 ^b	---	---
S95	290 ± 2 ^d	317.3 ± 1.3 ^c	383.5 ± 1.4 ^e	402.4 ± 1.1 ^b
PCL	---	---	374.1 ± 0.2 ^c	408.7 ± 0.2 ^c
S-H ₂ O	293.1 ± 0.8 ^{de}	320.92 ± 0.12 ^d	378 ± 2 ^d	410.8 ± 0.8 ^d
S-AA	293.0 ± 0.6 ^{de}	320 ± 0.2 ^d	378.0 ± 0.6 ^d	410.40 ± 0.12 ^d
S-PS	272.3 ± 0.7 ^b	299.9 ± 0.4 ^a	370.6 ± 0.6 ^b	403.4 ± 0.4 ^b
S95-H ₂ O	298.03 ± 0.13 ^e	319.4 ± 0.6 ^d	377.51 ± 0.11 ^d	409.90 ± 0.12 ^{cd}
S95-AA	295 ± 2 ^{de}	319.5 ± 1.2 ^d	376.5 ± 1.3 ^{cd}	408.9 ± 0.6 ^c
S95-PS	262 ± 2 ^a	300.9 ± 0.4 ^a	364 ± 2 ^a	399.75 ± 0.11 ^a

666
 667 Different superscript letters within the same column indicate significant differences among formulations (p < 0.05).

668
 669
 670
 671
 672
 673
 674
 675
 676

677 Table 3.- Mean values and standard deviation of mechanical properties of films equilibrated at 53% RH and 25 °C for 1 week (initial) and 5 weeks (final).

Films	EM (MPa)		TS (MPa)		E (%)	
	Initial	Final	Initial	Final	Initial	Final
S	324 ± 48 ^{e1}	587 ± 65 ^{e2}	10 ± 2 ^{d1}	15.7 ± 1.2 ^{e2}	28 ± 10 ^{c1}	4.1 ± 0.4 ^{a2}
S95	48 ± 10 ^{a1}	103 ± 10 ^{a2}	5.4 ± 1.5 ^{a1}	7.8 ± 0.7 ^{b2}	53 ± 5 ^{e1}	39 ± 5 ^{f2}
PCL	304 ± 11 ^{e1}	314 ± 51 ^{d1}	---	---	---	---
S-H ₂ O	215 ± 17 ^{d1}	284 ± 35 ^{d2}	9.1 ± 0.7 ^{c1}	11.9 ± 1.2 ^{d2}	15 ± 2 ^{ab1}	15 ± 5 ^{cd1}
S-AA	181 ± 16 ^{c1}	205 ± 33 ^{c1}	8.7 ± 1.0 ^{c1}	9.9 ± 0.6 ^{c2}	17 ± 4 ^{ab1}	17 ± 5 ^{d1}
S-PS	170 ± 16 ^{c1}	202 ± 18 ^{c2}	6.7 ± 0.6 ^{b1}	7.7 ± 1.0 ^{b2}	11 ± 5 ^{a1}	9 ± 4 ^{b1}
S95-H ₂ O	129 ± 17 ^{b1}	311 ± 14 ^{d2}	6.7 ± 0.6 ^{b1}	6.7 ± 1.0 ^{a1}	18 ± 5 ^{b1}	6.1 ± 0.6 ^{a2}
S95-AA	114 ± 14 ^{b1}	213 ± 5 ^{c2}	8.1 ± 0.9 ^{c1}	7.5 ± 0.6 ^{ab2}	35 ± 6 ^{d1}	12 ± 5 ^{bc2}
S95-PS	126 ± 27 ^{b1}	153 ± 30 ^{b1}	8.5 ± 1.0 ^{c1}	9 ± 2 ^{c1}	32 ± 8 ^{cd1}	27 ± 6 ^{e1}

678
 679 Different superscript letters within the same column indicate significant differences among formulations (p < 0.05).

680 Different superscript numbers within the same row indicate significant differences due to storage time (p < 0.05).

681

682

683

684

685

686

687

688 Table 4.- Mean values and standard deviation of water vapour permeability (WVP) and oxygen permeability (OP) of the different films at 1 (Initial time) and 5 (Final time)
 689 weeks of storage at 53% relative humidity and 25 °C.

Films	WVP (g·mm·kPa ⁻¹ ·h ⁻¹ ·m ²)		OP · 10 ¹⁴ (cm ³ ·m ⁻¹ ·s ⁻¹ ·Pa ⁻¹)	
	Initial	Final	Initial	Final
S	18.1 ± 1.4 ^{c1}	16 ± 2 ^{d1}	< D.L.	< D.L.
S95	20.41 ± 0.02 ^{d1}	18 ± 2 ^{e1}	12.2 ± 0.8 ^{a1}	19 ± 3 ^{ab2}
PCL	0.120 ± 0.04 ^{a1}	0.117 ± 0.011 ^{a1}	> D.L.	> D.L.
S-H ₂ O	0.8 ± 0.3 ^{ab1}	0.43 ± 0.07 ^{a1}	12 ± 2 ^{a1}	11.2 ± 1.5 ^{a1}
S-AA	0.71 ± 0.07 ^{ab1}	0.57 ± 0.07 ^{a1}	15 ± 2 ^{a1}	9 ± 3 ^{a1}
S-PS	0.7 ± 0.2 ^{ab1}	0.63 ± 0.07 ^{a1}	< D.L.	< D.L.
S95-H ₂ O	1.4 ± 0.3 ^{b1}	6.0 ± 0.5 ^{c2}	28 ± 5 ^{b1}	15.6 ± 1.0 ^{b2}
S95-AA	1.5 ± 0.6 ^{b1}	2.4 ± 0.9 ^{b1}	14 ± 3 ^{a1}	10 ± 2 ^{a1}
S95-PS	0.96 ± 0.04 ^{ab1}	1.24 ± 0.15 ^{ab2}	< D.L.	< D.L.

690
 691 D.L.: 0.1-200 cc/(m².day)
 692 Different superscript letters within the same column indicate significant differences among formulations (p < 0.05).
 693 Different superscript numbers within the same row indicate significant differences due to storage time (p < 0.05).

694
 695
 696
 697
 698

699 Table 5.- Mean values and standard deviation of surface roughness parameters and optical properties of the different films at 1 (Initial time) and 5 (Final time) weeks of
 700 storage at 53% relative humidity and 25 °C.

Films	Gloss (85°). Starch face		Gloss (85°). PCL face	
	Inicial	Final	Inicial	Final
S	40 ± 5 ^{c1}	37 ± 2 ^{c1}	---	---
S95	47 ± 11 ^{cd1}	25 ± 8 ^{b2}	---	---
PCL	---	---	59 ± 16 ^{e1}	57 ± 9 ^{c1}
S-H ₂ O	41 ± 5 ^{c1}	38 ± 9 ^{c1}	52 ± 9 ^{cde1}	39 ± 11 ^{b2}
S-AA	46 ± 7 ^{cd1}	39 ± 6 ^{c2}	52 ± 7 ^{cde1}	38 ± 13 ^{b2}
S-PS	51 ± 16 ^{de1}	43 ± 13 ^{c1}	54 ± 10 ^{de1}	39 ± 16 ^{b2}
S95-H ₂ O	16 ± 2 ^{ab1}	13 ± 2 ^{a2}	29 ± 5 ^{a1}	26 ± 8 ^{a1}
S95-AA	13 ± 4 ^{a1}	15 ± 8 ^{a1}	24 ± 5 ^{a1}	19 ± 10 ^{a1}
S95-PS	23 ± 2 ^{b1}	20 ± 6 ^{ab1}	45 ± 7 ^{bc1}	41 ± 9 ^{b1}

701
 702 Different superscript letters within the same column indicate significant differences among formulations (p < 0.05).

703 Different superscript numbers within the same row indicate significant differences due to storage time (p < 0.05).

704

705

706

707

708